



The Soret Effect in Dry Polymer Electrolyte

Journal:	<i>Molecular Systems Design & Engineering</i>
Manuscript ID	ME-ART-10-2019-000145.R1
Article Type:	Paper
Date Submitted by the Author:	14-Jan-2020
Complete List of Authors:	Mentor, Jesufane; FAMU-FSU College of Engineering, Chemical and Biomedical Engineering; Florida State University, Aero-propulsion, Mechatronics, and Energy Center Torres, Richard; FAMU-FSU College of Engineering, Chemical and Biomedical Engineering; Florida State University, Aero-propulsion, Mechatronics, and Energy Center Hallinan, Daniel; FAMU-FSU College of Engineering, Chemical and Biomedical Engineering; Florida State University, Aero-propulsion, Mechatronics, and Energy Center

SCHOLARONE™
Manuscripts

Design, System, Application paragraph

The desired system functionality pertains to converting waste heat to electricity and/or improving the efficiency of batteries. The system is based on a thermogalvanic cell that combines the properties of a battery with those of a thermoelectric. The design strategy relies on the fact that large thermal diffusion effects have been observed in polymer-based mixtures and extends the study of this effect to polymer electrolyte. Polymer electrolytes are of particular interest for the study of thermal diffusion (and application to thermogalvanics) because they are the first system in which the solvent is a high molecular weight polymer (with low mobility) and the salt alone can respond to the thermal gradient. An additional advantage of the molecular system design is that the material is solid, preventing the problem of convection that is often encountered in thermal diffusion studies. Since over half of energy produced is lost as heat, a technology for converting heat into something more useful, like electricity, would have a huge impact on energy sustainability.

ARTICLE

The Soret Effect in Dry Polymer Electrolyte

Jesufane Jenny Mentor,^a Richard Torres,^a and Daniel T. Hallinan Jr.*^a

Received 00th January 20xx,
Accepted 00th January 20xx

DOI: 10.1039/x0xx00000x

The Soret Effect results in a concentration gradient when a mixture is exposed to a temperature gradient. It is a balance between diffusion of mass driven by the temperature gradient (thermal diffusion) and mass diffusion acting to remove the concentration gradient. Thus, the Soret Effect is measured at steady state. In this work, the Soret Effect was studied in a thermogalvanic cell with lithium metal electrodes and a dry polymer electrolyte composed of poly(ethylene oxide) and lithium bis-trifluoromethanesulfonylimide (LiTFSI). The concentration gradient was determined by measuring the voltage of the thermogalvanic cell. This was examined at several different temperature gradients and with four different salt concentrations. The Soret coefficient was found to be similar to that observed in small-molecule mixtures and electrolytes and significantly less than polymeric systems. An explanation for this unexpected result is proffered. The Soret coefficient was found to be concentration dependent, which requires further investigation. Finally, it was demonstrated that the thermogalvanic cells used to measure the Soret coefficient can also be used to generate power. Thus, polymer electrolytes are potentially of interest for waste heat recovery, and thermal diffusion might be used to improve battery efficiency.

Introduction

According to the 2018 Lawrence Livermore National Laboratory energy flow diagram, more than two thirds of all energy produced in the United States was rejected.¹ This energy is rejected primarily in the form of heat. A cost-effective means to convert some of that heat to a usable form of energy, such as electricity, would have a profound impact on the nation's energy efficiency. One approach to directly convert heat to electricity is to take advantage of the temperature difference between a heat generating device (such as turbine exhaust in a power plant or vehicle exhaust) and the ambient atmosphere.

Thermoelectrics are a widely studied technology that relies on electron transport to convert temperature gradients to electricity.² These materials tend to be inorganic crystals containing rare earth elements,^{3,4} although polymeric hole/electron conductors are also being studied.⁵ Due to the strong temperature-dependence of thermoelectric performance, thermoelectric devices are usually operated with temperature gradients of hundreds of degrees. This

precludes them from being applied to recovery of low-grade waste heat, considered to be 125 °C or less.⁶

An alternative, for low-grade waste heat recovery, is thermogalvanic cells that rely on ion transport due to the Soret Effect and an electrochemical reaction to generate electricity. This fundamentally different process raises the question of how such devices will perform. Perhaps more interesting is the possibility that such cells present in studying the Soret Effect.

The Soret Effect arises when a temperature gradient is imposed on a multicomponent system, inducing a concentration gradient. The Soret Effect, also known as thermal diffusion, was first observed in 1856 by Ludwig,⁷ but was not studied comprehensively until 1879, when Charles Soret performed a set of careful experiments on aqueous salt solutions.⁸ Each solution was contained in a sealed glass tube with one end in a hot water bath and the other end in a cold water bath. He found that, after sufficient equilibration time, the salt concentration at the cold end of the tube was greater than that at the hot end. This was true for several different salts. Since then this effect has been examined in gas mixtures,⁹ liquid solutions,¹⁰⁻¹⁵ and polymer blends.¹⁶⁻¹⁸ Despite these efforts, there is not a comprehensive theory of the Soret Effect that applies to all the systems and conditions that have been studied. In fact, no single theory has been successful at universally predicting the *direction* of thermal diffusion

^a Florida A&M University-Florida State University College of Engineering, Department of Chemical and Biomedical Engineering, 2525 Pottsdamer Street, Tallahassee, FL 32310.

^b Aero-Propulsion, Mechatronics, and Energy Center, Florida State University, 2003 Levy Avenue, Tallahassee, FL 32310.

* Corresponding author email: dhallinan@eng.famu.fsu.edu

for all systems studied and for small and large temperature gradients.^{19, 20} Therefore, study of a new system type is reported here in which the matrix is a high molar mass polymer and the minority component is a salt. This mixture is termed a polymer electrolyte. Due to lack of optical transparency, a different approach to measuring the Soret effect is necessary.

Thermal diffusion measurements of neutral polymer blends suggest that a polymer-electrolyte-based thermo-electrochemical cell will have a significantly higher Soret response than liquid mixtures.¹⁸ This, coupled with low thermal conductivity of polymer electrolyte, makes it of practical interest. Polymer electrolytes have been studied extensively for use in lithium batteries.²¹ Polymers such as poly(ethylene oxide) (PEO) have functional groups that coordinate ions and thereby dissociate salt. A polymer electrolyte is an interesting system in which to study the Soret Effect for several reasons.

First, their solid-like nature prevents complications of convection that can be a large source of error in liquid systems.^{11, 22-24} Flow is expected to be negligible in this work, due to the polymer electrolyte having a viscosity on the order of 10^6 Poise.²⁵ Flow due to natural convection is further suppressed by aligning the temperature gradient parallel but in the opposite direction of gravity.

Second, the dramatically different molar masses (and therefore mobility) of the polymer and the ions could provide new insight into the Soret Effect. One theory predicts that mobility can be used to describe the Soret effect.²⁶ Polymer electrolytes provide a system in which the mobility of the components are dramatically different and in which the species solvating the ions (polymer segments) cannot transfer with the ion.

Finally, redox active ions enable electrochemical measurements to be used to sensitively probe concentration gradients induced by applied temperature gradients. This approach is an alternative to conventional, laser-based techniques.²⁷⁻²⁹ It can be applied to opaque or translucent mixtures, such as polymer electrolytes. By using the electrochemical cell described below, one can measure the electrical signal generated by thermally induced concentration gradients both to determine the Soret coefficient and to measure the amount of power that can be generated from the temperature gradient.

The hope is that these experimental measurements will be valuable to those refining thermal diffusion theory and incorporating thermal diffusion effects into battery models, e.g. to improve efficiency.

Experimental

Materials

400,000 g/mol PEO with 1000 ppm of butylated hydroxytoluene (BHT), anhydrous n-methyl-2-pyrrolidone (NMP), and acetone were used from Sigma Aldrich. Battery-grade lithium bis(trifluoromethanesulfonyl)imide (LiTFSI) salt from BASF was dried at 120°C for 48 hours under vacuum and transferred to an argon-filled glovebox (0.1 ppm H₂O and O₂) without being exposed to air. Flame-retardant garolite (G10) spacers (McMaster Carr, 254 μm thick) were used to hold the polymer electrolyte in place and add thermal insulation to impede heat transfer from heating plate to cooling plate. Lithium electrodes (MTI, Inc.) were punched as discs. Nickel tabs (TOB New Energy Limited), which are placed on the electrodes, were used as current collectors. Laminated aluminum pouch (MTI, Inc.) was used to vacuum seal the cell to prevent exposure to air while maintaining electrical contact between the nickel tabs, the electrodes, and the polymer electrolyte.

Material Preparation

Purifying PEO

PEO was separated from BHT to avoid any participation of BHT in electrochemical reactions. For the purification process, 1 g of PEO was added to 100 mL of acetone in a round bottom flask. The flask was connected to a condensing column, and both were purged with nitrogen. The acetone and PEO were stirred and heated to 50 °C for 3 hours. Next, the PEO was allowed to recrystallize at 0 °C and slowly warm to room temperature overnight. The precipitated PEO was vacuum filtered to maximize recovery. This process was repeated twice more and then the PEO was dried at 60 °C under vacuum overnight, before being transferred into an argon-filled glove box.

Electrolyte preparation

PEO and LiTFSI were dissolved in NMP at different molar ratios, r , of 0.0133, 0.0325, 0.0850, 0.1027 lithium salt to ethylene oxide repeat units (EO) [$\text{mol}_{\text{Li}}/\text{mol}_{\text{EO}}$]. r is readily converted to molality, $m = r/M_{\text{EO}}$, with the molar mass of EO ($M_{\text{EO}} = 44.053 \text{ g/mol}$). The corresponding molalities are 0.234, 0.738, 1.93, and 2.33 $\text{mol}_{\text{Li}}/\text{kg}_{\text{EO}}$. To achieve a well-mixed solution, the solution was stirred at 40 °C overnight, which resulted in a clear, viscous solution. The solution was cast on nickel foil at 60 °C, and the NMP allowed to evaporate. After 12 hours, the resulting clear solid membrane was peeled from the foil and dried at 90 °C under vacuum for 12 hours.

Electrochemical Cell Assembly

The membrane was placed in the center of a 1/4 inch diameter hole machined in the center of a G10 spacer. The thickness of the membrane was approximately the same thickness as the spacer. At 90 °C, the G10 spacer with the polymer electrolyte in the center was hot pressed for 30 seconds. Any excess polymer on the surface of the spacer was scraped off. Lithium electrodes were punched with a diameter of 7/16 inch and pressed to each side of the membrane. Then nickel tabs were placed on top of the lithium electrodes with Kapton tape holding them in place. The symmetric cell was then vacuum sealed in an aluminum pouch prior to being removed from the glove box.

Testing

Electrochemical Break-in

The symmetric cell was connected to a Biologic VMP3 and heated to 80 °C. To ensure thermal equilibration, the open circuit voltage (OCV) of the cell was measured every 30 seconds for 2 hours. Then impedance spectroscopy was conducted at an initial frequency of 1 MHz to a final frequency of 100 mHz. Next, a current of 1 μA was applied to the cell for 30 minutes. This break-in protocol was found to be important to obtain reproducible OCV near zero, which indicated good contact between the lithium electrodes and the polymer electrolyte.

Soret Measurements

The cell was next placed in a custom set-up depicted in Figure 1. A feedback-controlled electrically heated plate was on top of the cell, and a Peltier-cooled plate

(TE Technology, Inc) was beneath the cell. Temperature was measured with two fine-gauge surface thermocouples (K-type with an Omega data logger, accuracy $\pm 0.35 \text{ }^\circ\text{C}$) located in a dummy cell lacking lithium electrodes and polymer electrolyte. The dummy cell had approximately the same thickness as the electrochemical cell so that the temperature measurements were an accurate representation of the temperature at the polymer electrolyte-electrode interfaces.

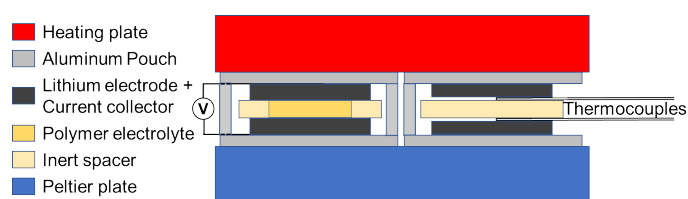


Figure 1. Schematic of the experimental set-up for measuring the Soret coefficient electrochemically.

A small section of the outer insulation of the aluminum pouch was removed and the pouch grounded so that a Faraday shield was created. This shield was important to minimize the noise in the voltage measurements that are sensitive to the electrical fields generated by the heating and cooling elements.

Soret measurements were conducted at an average temperature of 80 °C. At each applied temperature gradient, voltage was measured with a Keithley 2401 SourceMeter until steady state was reached, approximately 8 hours. The set temperature of the hot side was incrementally increased by 5 °C and the set temperature of the cold side was incrementally decreased 5 °C every 8 hours until the Peltier temperature was 65 °C and the heating plate temperature was 95 °C. Experiments below 65 °C were not attempted in order to avoid crystallization of the polymer electrolyte,³⁰ which might complicate the heat and mass transport mechanisms.^{92, 93} The reported temperature differences were calculated from the actual temperatures measured in the dummy cell. The actual temperature difference was significantly less than the difference of the set temperatures, due to parasitic heat transfer through various components of the set-up.

Power Measurements

At each applied temperature gradient after the cell reached steady-state, a voltage sweep was conducted from 0 V to the measured steady-state OCV. The current was measured, and power was calculated from the applied voltage and measured current.

Theory

The response of thermo-electrochemical cells is based on two principles. The first is the Soret Effect, also known as thermal diffusion in molecular mixtures or thermophoresis in colloidal dispersions. Note that in this context thermal diffusion refers to *mass* diffusion driven by a temperature gradient, *not* diffusion of thermal energy. The second principle is that a concentration gradient in an electrolyte induces an electrical potential in an electrochemical cell, which in the absence of current can be written³¹

$$FU = (1 - t_+^0)(\mu_A^{(2)} - \mu_A^{(1)}). \quad (1)$$

F is Faraday's constant. The transference number, t_+^0 , is the fraction of charge carried by the reactive ions (cations in this work). It is assumed to be constant over the electrochemical potential range in Equation 1. The difference of electrochemical potential of the salt at electrode 2, $\mu_A^{(2)}$, versus that at electrode 1, $\mu_A^{(1)}$, induces an electrical potential, U , which is often termed a junction potential or concentration overpotential. For more detail, refer to section 2.6 of reference³¹.

The Soret coefficient is a constant that embodies the balance between thermal diffusion and Fickian diffusion. The diffusive mass flux of species A , \mathbf{j}_A , in a binary mixture (referenced to a mass average velocity) has been written in various forms. One form is

$$\mathbf{j}_A = -\rho[D_{AB}\nabla\omega_A + D_T\nabla\ln T], \quad (2)$$

where ρ is density. The first term is from Fick's first law (including the Fickian diffusion coefficient, D_{AB} , and the gradient of mass fraction, $\nabla\omega_A$). The second term accounts for thermal diffusion (including the thermal diffusion coefficient, D_T , and the gradient of the natural logarithm of temperature, $\nabla\ln T$). Both diffusion coefficients having units of length squared per time. A more appropriate form, derived from irreversible

thermodynamics, is symmetric in two components (A and B),^{32, 33} such that

$$\mathbf{j}_A = -\rho[D_{AB}\nabla\omega_A + D_T\omega_A\omega_B\nabla\ln T]. \quad (3)$$

This form accounts explicitly for the concentration dependence predicted by theory and approximately for that observed in experiments.⁹ Unfortunately, there is no universal convention used to define the thermal diffusion coefficient, such that at least two other forms of the thermal diffusion flux have been used. Perhaps the most pronounced example of this is that studies of thermal diffusion in gases have used expressions similar to equations 2 and 3, whereas in condensed systems temperature dependence has been lumped into the thermal diffusion coefficient, as follows:

$$\mathbf{j}_A = -\rho[D_{AB}\nabla\omega_A + D_T\omega_A\omega_B\nabla T]. \quad (4)$$

In this case, D_T has units of, for example, $\text{cm}^2/\text{K s}$. At steady state, the flux is zero if the cell is at open circuit; so that the Soret coefficient ($S_T = D_T/D_{AB}$) can be determined from a set of steady-state measurements of the concentration difference across the mixture ($\Delta\omega_A$) versus the temperature difference across the mixture (ΔT). Depending on which convention is adopted, it will take one of the following forms.

$$S_T \propto \frac{\Delta\omega_A}{\Delta\ln T} \text{ or } \frac{\Delta\ln(\omega_A/\omega_B)}{\Delta\ln T} \text{ or } \frac{\Delta\ln(\omega_A/\omega_B)}{\Delta T} \text{ or } \frac{\Delta\omega_A}{\Delta T} \quad (5)$$

In integrating across the mixture, these expressions have assumed that S_T is constant at the mean temperature.³⁴ The first two expressions of equation 5 have conventionally been employed in gases, and the dimensionless number, S_T , referred to as the thermal diffusion factor. In condensed phases, convention is to report S_T with units of K^{-1} , such that the 3rd or 4th expression is appropriate, although the 4th expression originally used by Soret is now considered incorrect.¹⁰ It is sometimes also assumed that the concentration difference is small enough to use

$$S_T = \frac{1}{\omega_A^0\omega_B^0} \frac{\Delta\omega_A}{\Delta T} = \frac{1}{x_A^0x_B^0} \frac{\Delta x_A}{\Delta T} = \frac{1}{m^0} \frac{\Delta m}{\Delta T}, \quad (6)$$

where ω_i^0 is taken as the equilibrium mass fraction of component i . By working in molar flux units (referenced to a molar-averaged velocity), the Soret coefficient can equivalently be related to mole

fractions or even molality, $m = \frac{x_A}{x_B M_B}$ where A is considered solute and B solvent.

D_T and S_T can be either positive or negative. If A is the higher molecular weight component, then the coefficients tend to be greater than zero, and A tends to move from hot to cold. Due to conservation of mass, $D_T(A) = -D_T(B)$.³⁵ However, thermal diffusion is sensitive to interaction in the mixture, such that a reversal of sign has been observed with a change in equilibrium concentration.^{19, 20} Although the salt is the lower molecular weight component, it is also essentially the only component that can move on the timescale of these experiments, due to the high molecular weight of the PEO. Furthermore, strong complex interactions are known to exist between PEO and lithium salts. Thus, it will be interesting to see the direction of thermal diffusion, i.e. the sign of the Soret coefficient.

Results and Discussion

Steady-state voltage measurements as a function of temperature gradient are shown in Figure 2. The slope is an apparent Seebeck coefficient, the values of which are reported in Table 1. As described below, this is primarily caused by the concentration gradient that develops in the polymer electrolyte due to the Soret Effect. However, there is a small actual Seebeck contribution to the cell voltage due to the lithium electrode-nickel current collector junctions being subjected to a temperature gradient.^{63, 66-67} Based on values reported in literature for lithium and nickel this amounts to $-8 \mu\text{V/K}$,³⁶⁻³⁹ which is less than 10% of the apparent Seebeck coefficient due to the Soret Effect.

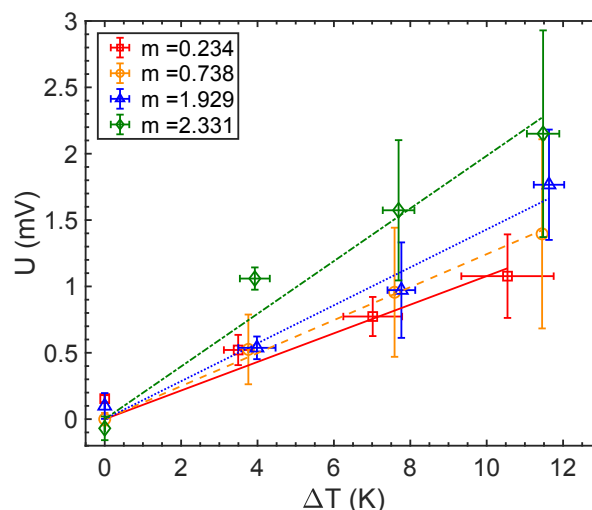


Figure 2. Measured cell voltage, U , versus temperature difference across electrolyte at an average temperature of $80 \text{ }^\circ\text{C}$ for salt molalities noted in legend. Linear regressions with intercept fixed to the origin are shown. Error bars are one standard deviation based on measurements of at least two cells.

Table 1. Apparent Seebeck coefficients, transference numbers, and Soret coefficients. Standard error of linear regression is reported for Seebeck and Soret coefficients. Error reported in reference⁴⁰ is given for transference number.

m^0 [mol _{salt} /kg _{EO}]	$U/\Delta T$ [mV/K]	t_+^0	S_T [10^{-3} K^{-1}]
0.234	0.11 ± 0.01	0.07 ± 0.02	-3.4 ± 0.3
0.738	0.124 ± 0.003	0.3 ± 0.1	-5.5 ± 0.1
1.929	0.143 ± 0.008	0.37 ± 0.06	-6.7 ± 0.4
2.331	0.20 ± 0.01	0.20 ± 0.05	-7.3 ± 0.5

For a monovalent binary electrolyte in terms of salt molality, m , equation 1 can be written

$$U = \frac{RT}{F} t_-^0 \ln \left(\frac{m^{(2)} \gamma_{\pm}^{(2)}}{m^{(1)} \gamma_{\pm}^{(1)}} \right). \quad (7)$$

R is the gas constant and T is absolute temperature. This expression relies on the fact that the transference numbers of cations and anions (t_{\pm}^0) sum to unity. $m^{(n)}$ refers to the salt molality in the electrolyte near the interface with electrode n . As first pointed out by de Groot,³² it is preferable to work in molality so that density differences due to the temperature gradient do not need to be considered. The activity coefficients, $\gamma_{\pm}^{(n)}$, account for deviation from ideality (having a value

of unity in an ideal electrolyte). If constant transport coefficients and ideal electrolytes are assumed, there is a linear concentration gradient at steady state. Taking $m^{(1)} = m^0 - \frac{\Delta m}{2}$ and $m^{(2)} = m^0 + \frac{\Delta m}{2}$, then

$$\Delta m = 2m^0 \left(\frac{\exp\left(\frac{FU}{RTt_-^0}\right) - 1}{\exp\left(\frac{FU}{RTt_-^0}\right) + 1} \right) = 2m^0 \tanh\left(\frac{FU}{2t_-^0 RT}\right). \quad (8)$$

Transference numbers, $t_-^0 = 1 - t_+^0$, are taken from Pesko, Balsara, and coworkers⁴⁰ and reported in Table 1. Steady-state potential measurements have been used to determine the concentration gradients that develop as a result of the temperature gradient.

The salt molality difference (Δm) is plotted against temperature differences (ΔT), in Figure 3a. The slope yields S_T according to:^{11, 18}

$$\Delta m = -S_T m^0 \Delta T. \quad (9)$$

Figure 3b presents the same analysis without assuming that the concentration gradient is small. In other words, $\ln\left(\frac{m^{(2)}}{m^{(1)}}\right)$ is plotted versus ΔT , where

$$\ln\left(\frac{m^{(2)}}{m^{(1)}}\right) = \frac{FU}{RTt_-^0} - \ln\left(\frac{\gamma_{\pm}^{(2)}}{\gamma_{\pm}^{(1)}}\right). \quad (10)$$

In this case, the negative of the slope yields S_T directly, if the electrolyte is ideal. The agreement between these two approaches is nearly perfect (at most 0.1% disagreement at the highest concentration investigated), indicating that the concentration gradients are indeed small. The measured concentration gradients range from 0.5% of m^0 at the lowest ΔT and m^0 to 7.9% of m^0 at the highest ΔT and m^0 . S_T at each m^0 are reported in Table 1.

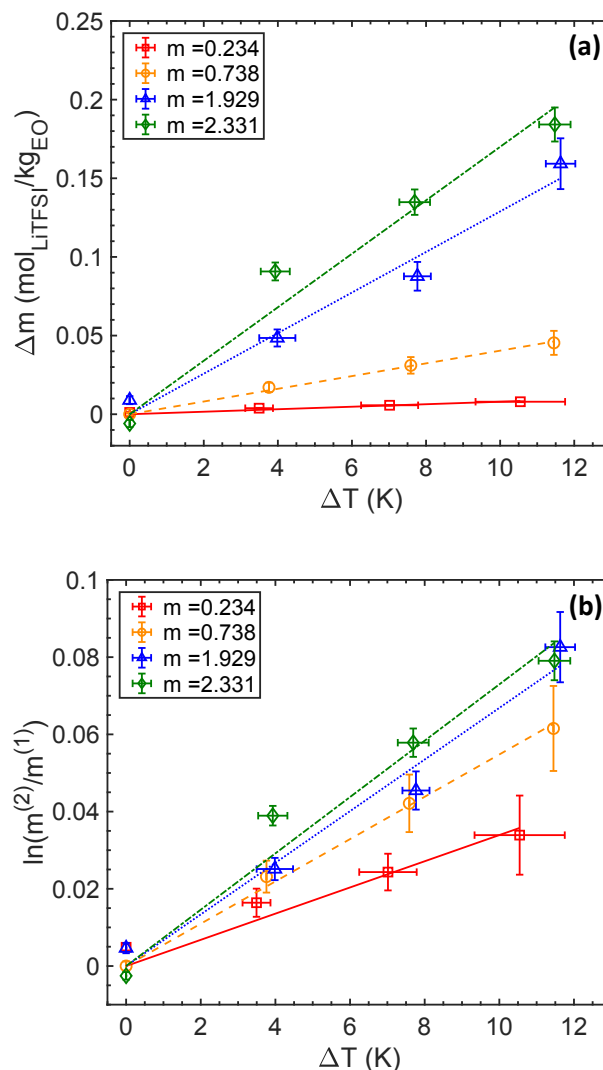


Figure 3. (a) Linear concentration difference across electrolyte, Δm , calculated from measured cell voltage using equation 8 as a function of temperature difference across polymer electrolyte. Linear regressions with intercept fixed to the origin are shown. (b) Log concentration difference across electrolyte, calculated according to equation 10, as a function of temperature difference across cell. Linear regressions of S_T are shown. Error bars are one standard deviation based on propagation of U and t_+^0 error.

Values of S_T for the salt are negative indicating that the salt moves from the cold to the hot electrode, i.e. salt concentrates on the hotter side of the polymer electrolyte. Being the lower molar mass component in the polymer electrolyte mixture, the direction of thermal diffusion of the salt agrees with what has been observed in small-molecule mixtures. It was not obvious that this would be the case. Transport of ions in polymer electrolyte, e.g. Fickian diffusion of salt, is known to be coupled to segmental motion of the polymer. In other words, it is not necessary for entire polymer chains to move. In fact, based on the reported

self-diffusion coefficient of PEO (295 kg/mol, 100 °C), it would take 4 years for a PEO chain to diffusion across the 254 μm thick polymer electrolyte.⁴¹ Rather, rearrangement of short segments of polymer chains is sufficient for long-range transport of ions (and other small molecules).

This provides some insight into the magnitude of the Soret coefficients measured in this work. The values reported here are much closer to small molecule mixtures (liquids and aqueous electrolytes, $S_T \sim 0.001 - 0.01 \text{ K}^{-1}$)¹⁰⁻¹⁵ than they are to polymer blends ($S_T \sim 0.1 \text{ K}^{-1}$)¹⁶ and polymer solutions ($S_T \sim 1 \text{ K}^{-1}$).^{26, 42-46} The expectation of a large Soret coefficient in polymer electrolyte is clearly not supported by these results. It is worth noting that S_T diverges to large values in polymer blends near a critical point (0.3 to 20 K^{-1}).¹⁸ It remains to be seen if approaching a critical point will result in similar large increases in S_T in dry polymer electrolytes.

The Soret coefficient values being lower than expected adds quite an interesting data set to the body of work on Soret coefficients. The apparent discrepancy between these results and those of polymer blends and solutions can be explained by considering the fact that in polymer blends and polymer solutions, the polymer chains are diffusing on the time scale of the experiments. However, in this work it is only the salt that is experiencing long-range diffusion, mitigated by segmental motion of the polymer matrix. This predicts that S_T will not be dependent on the molar mass of the polymer matrix in polymer electrolytes (or any system in which a small molecule is diffusing through a high molar mass polymer matrix). This prediction is in contrast to studies of polymer solutions, in which S_T is molar mass dependent due to the molar mass dependence of the polymer diffusion coefficient.²⁶ The prediction will be evaluated in future work.

The Soret coefficients in Table 1 increase with increasing equilibrium salt concentration. This is a surprising result since S_T of charged colloids has been found to *decrease* with decreasing Debye screening length (which is inversely proportional to salt concentration).⁴⁷ In polymer electrolytes, ion mobility is known to decrease with increasing salt concentration.²¹ Since S_T is the ratio of thermal diffusion and Fickian diffusion, a decrease of Fickian mobility with increasing salt concentration could explain the increase of S_T . It is unclear at this point if the apparent concentration

dependence of S_T is due to the neglected activity coefficient term or is inherent to S_T . Direct spectroscopic measurements of concentration gradients are underway to address this question.

Returning to practical evaluation of polymer-electrolyte-based thermogalvanic cells, the apparent Seebeck values reported in Table 1 are of similar magnitude to actual Seebeck coefficients of organic semiconductors being studied for thermoelectrics⁴⁸ and bismuth-telluride-based compounds,⁴⁹ but they slightly surpass other inorganic semiconductors like reduced graphene oxide that has values up to 60 $\mu\text{V}/\text{K}$.⁵⁰ Comparing to materials that operate at significantly higher temperatures, the apparent Seebeck values of the dry polymer electrolyte are also of similar magnitude to top performing metal alloys (at 650 to 800 K).⁵¹ The low values of t_+^0 in the polymer electrolyte balance the rather low values of S_T , resulting in reasonable Seebeck performance of the thermogalvanic cell.

Power measurements were also conducted after establishing steady state to demonstrate that these devices can indeed generate power. Representative voltage sweeps are shown in Figure S2, where both measured current and calculated power are reported. The maximum power generated by the thermogalvanic cells is reported in Figure 4 as a function of temperature gradient for each equilibrium salt concentration noted in the legend. Based on voltage sweeps in the absence of a temperature gradient, the power resolution is 0.006 nW/cm². Despite reasonable resolution, there is significant deviation between measurements and among samples. However, some rough trends can be discerned. First, the magnitude of P_{max} increases with increasing temperature gradient. Second, the most power is generated by $m = 1.929 \text{ mol}_{\text{LiTFSI}}/\text{kg}_{\text{PEO}}$, which is the polymer electrolyte concentration with highest ionic conductivity.³⁰ Thus, qualitatively there is analogy to thermoelectrics in that power is a function of driving force and carrier mobility. In contradistinction, thermogalvanic power appears to be a continuous function of temperature gradient, i.e. power decreases with temperature gradient but continues to be produced with exceptionally small gradients.

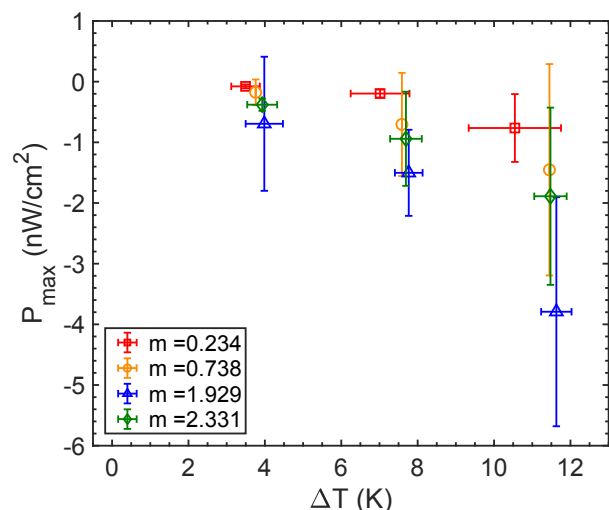


Figure 4. Maximum thermogalvanic power as a function of temperature gradient and equilibrium polymer electrolyte molality noted in legend.

Conclusions

Soret coefficients can be measured in symmetric thermogalvanic cells with simple voltage measurements, if certain simplifying assumptions are made. This approach was used in lithium symmetric cells containing polymer electrolyte (PEO and LiTFSI) with concentrations from **0.2 to 2.3 mol_{LiTFSI}/kg_{PEO}**. Soret coefficients were determined at steady state with temperature gradients of **3.8 K to 11.3 K**. They were found to be much closer to values of small molecule mixtures than to that of polymer systems in which the polymer chains are mobile. The presence of an immobilized matrix provides a system in which essentially only one component is experiencing thermal diffusion, which opens up the possibility of studying not only a wide range of salts, but also neutral molecules in polymers. Future work will evaluate the prediction that S_T is molar mass independent in entangled polymer matrices by examining thermal diffusion in a wide range of PEO molar masses. The Soret coefficient also appears to have an unexpected concentration dependence. Decrease of ion mobility with increasing salt concentration could explain this observation, once thermodynamic non-ideality is ruled out with spectroscopic measurements that are underway.

Much work remains to fully understand thermal diffusion in polymer electrolytes. This work demonstrates that polymer electrolytes are an interesting system for such an investigation due to their having a Soret coefficient of similar magnitude to small molecule mixtures. Furthermore, it has been demonstrated that a thermogalvanic cell is a feasible approach for studying thermal diffusion in opaque mixtures. Based on studies in neutral polymer systems, where mass and thermal diffusion diverge upon approaching a phase transition, it remains to be seen if more promising thermogalvanic performance will be observed when spanning a phase

transition in a polymer electrolyte. This could, for example, be realized by reducing the low temperature side to a point at which the polymer electrolyte is semi-crystalline. We also note in passing that with an understanding of thermal diffusion it might be possible to improve battery efficiency via intelligent temperature control.

Conflicts of interest

There are no conflicts to declare.

Acknowledgments

The authors acknowledge support from several sources over the life of this work, including the FSU Council on Research and Creativity (CRC) Planning Grant and NSF award 1804871. J.J.M. acknowledges support from the FAMU-FSU College of Engineering. R.T. acknowledges support from the FSU IDEA Grant. D.T.H. acknowledges partial support from NSF awards 1751450 and 1735968. This work would not have been possible without design and fabrication support from Jeremy Phillips and colleagues at the FAMU-FSU Engineering Machine Shop. Lindsey Hallinan is acknowledged for critical editing support.

Notes and references

1. LLNL-MI-410527, 2018.
2. A. Zevkink, D. M. Smiadak, J. L. Blackburn, A. J. Ferguson, M. L. Chabinyk, O. Delaire, J. Wang, K. Kovnir, J. Martin, L. T. Schelhas, T. D. Sparks, S. D. Kang, M. T. Dylla, G. J. Snyder, B. R. Ortiz and E. S. Toberer, *Applied Physics Reviews*, 2018, **5**, 021303.
3. Y. Pei, H. Wang and G. J. Snyder, *Advanced Materials*, 2012, **24**, 6125-6135.
4. Y. Lan, A. J. Minnich, G. Chen and Z. Ren, *Advanced Functional Materials*, 2010, **20**, 357-376.
5. O. Bubnova and X. Crispin, *Energy & Environmental Science*, 2012, **5**, 9345-9362.
6. D. M. Rowe, in *XVII International Conference on Thermoelectrics, Proceedings ICT 98*, IEEE, 1998, DOI: 10.1109/ict.1998.740309, pp. 18-24.
7. C. Ludwig, *Sitz. Ber Akad. Wiss. Wien Math-Naturw. Kl.*, 1856, **20**, 539.
8. C. Soret, in *ARCHIVES DES SCIENCES PHYSIQUES ET NATURELLES*, Imprimerie Charles Schuchardt, GENÈVE, 1879, pp. 48-61.
9. K. E. Grew and T. L. Ibbs, *Thermal Diffusion in Gases*, Cambridge University Press, London, 1952.
10. H. J. V. Tyrrell, *Diffusion and heat flow in liquids*, Butterworth, London, 1961.
11. J. K. Platten, *Journal of Applied Mechanics-Transactions of the ASME*, 2006, **73**, 5-15.
12. S. Hartmann, G. Wittko, W. Koehler, K. I. Morozov, K. Albers and G. Sadowski, *Physical Review Letters*, 2012, **109**.
13. A. Koeniger, B. Meier and W. Koehler, *Philosophical Magazine*, 2009, **89**, 907-923.
14. J. Luettmer-Strathmann and J. V. Sengers, *Journal of Chemical Physics*, 1996, **104**, 3026-3047.

15. D. G. Leaist, *Journal of Solution Chemistry*, 1990, **19**, 1-10.
16. W. Koehler, A. Krekhov and W. Zimmermann, in *Complex Macromolecular Systems I*, eds. A. H. E. Muller and H. W. Schmidt, 2010, vol. 227, pp. 145-198.
17. S. Wiegand, *Journal of Physics-Condensed Matter*, 2004, **16**, R357-R379.
18. W. Enge and W. Kohler, *Physical Chemistry Chemical Physics*, 2004, **6**, 2373-2378.
19. R. Kita, G. Kircher and S. Wiegand, *Journal of Chemical Physics*, 2004, **121**, 9140-9146.
20. R. Kita, S. Wiegand and J. Luettmmer-Strathmann, *Journal of Chemical Physics*, 2004, **121**, 3874-3885.
21. D. T. Hallinan and N. P. Balsara, *Annual Review of Materials Research*, 2013, **43**, 503-525.
22. A. Gunawan, C.-H. Lin, D. A. Buttry, V. Mujica, R. A. Taylor, R. S. Prasher and P. E. Phelan, *Nanoscale and Microscale Thermophysical Engineering*, 2013, **17**, 304-323.
23. M. Martin, B. R. Min and M. H. Moon, *Journal of Chromatography A*, 1997, **788**, 121-130.
24. A. Regazzetti, M. Hoyos and M. Martin, *Analytical Chemistry*, 2004, **76**, 5787-5798.
25. A. Teramoto and H. Fujita, *Die Makromolekulare Chemie*, 1965, **85**, 261-272.
26. J. Chan, J. J. Popov, S. Kolisnek-Kehl and D. G. Leaist, *Journal of Solution Chemistry*, 2003, **32**, 197-214.
27. C. Allain and P. Lallemand, *Comptes Rendus Hebdomadaires Des Seances De L Academie Des Sciences Serie B*, 1977, **285**, 187-190.
28. S. Wiegand and W. Kohler, in *Thermal Nonequilibrium Phenomena in Fluid Mixtures*, eds. W. Kohler and S. Wiegand, 2002, vol. 584, pp. 189-210.
29. W. Kohler and R. Schafer, *New Developments in Polymer Analytics II*, 2000, **151**, 1-59.
30. S. Lascaud, M. Perrier, A. Vallee, S. Besner, J. Prudhomme and M. Armand, *Macromolecules*, 1994, **27**, 7469-7477.
31. J. Newman and K. E. Thomas-Alyea, *Electrochemical Systems*, Wiley-Interscience, Hoboken, NJ 3rd edn., 2004.
32. S. R. De Groot, *Physica*, 1942, **9**, 699-708.
33. S. Chapman and J. Larmor, *Philosophical Transactions of the Royal Society of London. Series A, Containing Papers of a Mathematical or Physical Character*, 1918, **217**, 115-197.
34. R. B. Bird, W. E. Stewart and E. N. Lightfoot, *Transport Phenomena*, John Wiley & Sons, New York, 1960.
35. W. M. Deen, *Analysis of Transport Phenomena*, Oxford University Press, 2 edn., 2011.
36. B. Xu and M. J. Verstraete, *Physical Review Letters*, 2014, **112**.
37. V. Surla, M. Tung, W. Xu, D. Andruczyk, M. Neumann, D. N. Ruzic and D. Mansfield, *Journal of Nuclear Materials*, 2011, **415**, 18-22.
38. K. E. Grew, *Physical Review*, 1932, **41**, 356-363.
39. X. Zhang, A. Cramer, A. Lange and G. Gerbeth, *Magnetohydrodynamics*, 2009, **45**, 25-42.
40. D. M. Pesko, K. Timachova, R. Bhattacharya, M. C. Smith, I. Villaluenga, J. Newman and N. P. Balsara, *Journal of The Electrochemical Society*, 2017, **164**, E3569-E3575.
41. M. Appel and G. Fleischer, *Macromolecules*, 1993, **26**, 5520-5525.
42. E. Bringuier and A. Bourdon, *Physical Review E*, 2003, **67**.
43. B. J. de Gans, R. Kita, B. Muller and S. Wiegand, *Journal of Chemical Physics*, 2003, **118**, 8073-8081.
44. J. Rauch and W. Kohler, *Journal of Chemical Physics*, 2003, **119**, 11977-11988.
45. C. VanBatten, M. Hoyos and M. Martin, *Chromatographia*, 1997, **45**, 121-126.
46. K. J. Zhang, M. E. Briggs, R. W. Gammon, J. V. Sengers and J. F. Douglas, *Journal of Chemical Physics*, 1999, **111**, 2270-2282.
47. S. Duhr and D. Braun, *Proceedings of the National Academy of Sciences of the United States of America*, 2006, **103**, 19678-19682.
48. M. H. Elsheikh, D. A. Shnawah, M. F. M. Sabri, S. B. M. Said, M. H. Hassan, M. B. A. Bashir and M. Mohamad, *Renewable & Sustainable Energy Reviews*, 2014, **30**, 337-355.
49. I. T. Witting, T. C. Chasapis, F. Ricci, M. Peters, N. A. Heinz, G. Hautier and G. J. Snyder, *Advanced Electronic Materials*, 2019, **5**, 1800904.
50. J. Choi, N. D. K. Tu, S.-S. Lee, H. Lee, J. S. Kim and H. Kim, *Macromolecular Research*, 2014, **22**, 1104-1108.
51. J. Li, W. Li, Z. Bu, X. Wang, B. Gao, F. Xiong, Y. Chen and Y. Pei, *ACS Applied Materials & Interfaces*, 2018, **10**, 39904-39911.